ACS APPLIED MATERIALS & INTERFACES

Research Article

www.acsami.org

Graphene Oxide-Promoted Reshaping and Coarsening of Gold Nanorods and Nanoparticles

Hanqing Pan, Serena Low, Nisala Weerasuriya, and Young-Seok Shon*

Department of Chemistry and Biochemistry, California State University, Long Beach, 1250 Bellflower Boulevard, Long Beach, California 90840, United States

Supporting Information

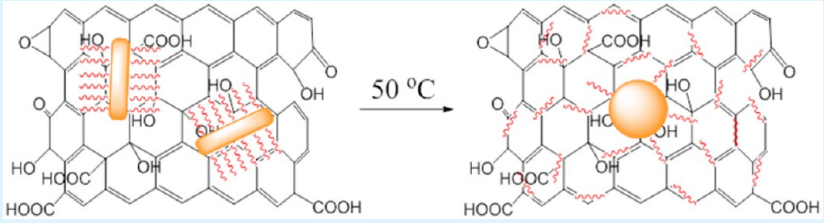

ABSTRACT: This paper describes thermally induced reshaping and coarsening behaviors of gold nanorods and nanoparticles immobilized on the surface of graphene oxide. Cetyltrimethylammonium bromide-stabilized gold nanorods with an aspect ratio of ~3.5 (54:15 nm) and glutathione-capped gold nanoparticles with an average core size of ~3 nm were synthesized and self-assembled onto the surface of graphene oxide. The hybrid materials were then heated at different temperatures ranging from 50 to 300 °C. The effects of heat treatments were monitored using UV−vis spectroscopy and transmission electron microscopy (TEM). These results were directly compared with those of heat-treated free-standing gold nanorods and nanoparticles without graphene oxide to understand the heat-induced morphological changes of the nanohybrids. The obtained results showed that the gold nanorods would undergo a complete reshaping to spherical particles at the temperature of 50 °C when they are assembled on graphene oxide. In comparison, the complete reshaping of free-standing gold nanorods to spherical particles would ultimately require a heating of the samples at 200 °C. In addition, the spherical gold nanoparticles immobilized on graphene oxide would undergo a rapid coarsening at the temperature of 100−150 °C, which was lower than the temperature (150−200 °C) required for visible coarsening of free-standing gold nanoparticles. The results indicated that graphene oxide facilitates the reshaping and coarsening of gold nanorods and nanoparticles, respectively, during the heat treatments. The stripping and spillover of stabilizing ligands promoted by graphene oxide are proposed to be the main mechanism for the enhancements in the heat-induced transformations of nanohybrids.

KEYWORDS: *nanorods, nanoparticles, graphene oxide, gold, reshaping, coarsening*

INTRODUCTION

Nanoparticle−graphene oxide hybrid materials not only retain individual properties of the nanoparticles and graphene oxide but also exhibit additional synergistic properties such as enhanced catalytic, magnetic, electrical, and optical activities.[1−3]

Maximizing their potentials by cross-coupling two unique nanomaterials could lead to several practical applications such as batteries, supercapacitors, fuel cells, photovoltaic devices, photocatalysis, sensors, and surface enhanced Raman scattering (SERS).[4−8] Recent studies also showed that metal nanoparticle−graphene oxide hybrid films might have a capability to replace indium tin oxide,[9] which is one of the important materials in semiconductor applications.

Despite being encapsulated by stabilizing ligands or surfactants, nanoscale metallic species obtained by bottom-up solution chemistry are often vulnerable to changes in size and shape when they are exposed to heat or light irradiation.[10,11] Especially, in the case of catalysis applications that prioritize the long-term activity and recyclability of metal nanoparticle catalysts, the use of solid supports such as silica and alumina was often necessary for kinetically trapping metal nanoparticles and enhancing their stability.[12,13] The adsorption of metal nanoparticles onto the surface of carbon allotropes including nanotube and graphene oxide is also postulated to enhance the overall stability of nanoparticle catalysts and often used as the strategy for various catalytic reactions.[14−19] However, systematic studies regarding the stability of nanoparticle−graphene oxide hybrid materials under elevated temperatures are currently lacking in the literature, despite the frequent use of annealing or calcination to remove surface adsorbed organic species from the nanoparticle surfaces for the activation of metal nanoparticle catalysts.[20−22]

In this study, the nanoparticle−graphene oxide hybrid materials were prepared by anchoring preformed gold nanorods and nanoparticles onto the surface of graphene oxide. It has been known that the presence of defects and oxygen functional

Received: December 12, 2014
Accepted: January 22, 2015
Published: January 22, 2015

DOI: 10.1021/am508801e
ACS Appl. Mater. Interfaces 2015, 7, 3406−3413

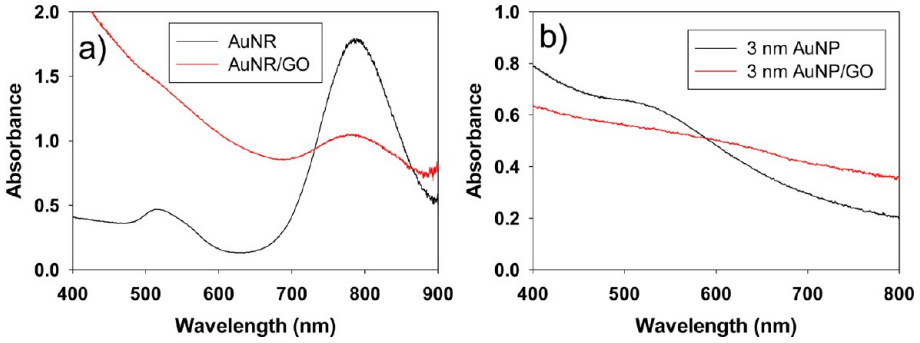

Figure 1. UV−vis spectra of (a) gold nanorods and (b) 3 nm gold nanoparticles before and after they are adsorbed onto the surface of graphene oxide.

groups make graphene oxide excellent templates for the postassembly of nanoparticles.[1] The nanorod− and nanoparticle−graphene oxide hybrid materials were then annealed from 50 to 300 °C to examine how the surface-immobilized nanorods and nanoparticles would undergo either reshaping to become spherical nanoparticles or coalescence to become larger particles, respectively. This study is to understand the nature and extent of the transformations (e.g., aggregation, coalescence, and migration) and to fully grasp on the role of graphene oxide in the stability of metal nanoparticles during the heat treatment. The improved understanding of such a thermally induced transformation of nanohybrid materials would contribute toward predicting materials performances in applications such as catalysis and optical device.

EXPERIMENTAL SECTION

Materials. The following materials were purchased from the indicated suppliers and used as received: hydrogen tetrachloroaurate trihydrate ($HAuCl_4 \cdot 3H_2O$) was purchased from Acros. Sodium citrate, silver nitrate, ascorbic acid, and graphene oxide were purchased from Sigma-Aldrich. Methanol, glutathione, and sodium borohydride ($NaBH_4$) were obtained from Fisher Scientific. (1-Cetyl)-trimethylammonium bromide (CTAB) was purchased from Alfa Aesar. Spectra/Por cellulose ester (CE) dialysis membranes (MW = 8000−10 000 Da) were purchased from Spectrum Laboratories, Inc. Nanopure water was purified by a Barnstead NANOpure Diamond ion exchange resins purification unit.

Synthesis of Surfactant-Stabilized Gold Nanorods. Gold nanorods were synthesized using the procedure reported by Russell et al. using a seed-mediated method.[23] In this method, a seed solution and a growth solution were mixed by introducing a small amount of seed solution to the growth solution, which initiates nanorod growth. Both a seed solution and a growth solution were prepared in 20 mL dram vials, which were cleaned with aqua regia, extensively rinsed, and annealed at 150 °C for 2 h prior to use. The aqueous seed solution consisted of 5.0 mL of 0.50 mM $HAuCl_4$ and 5.0 mL of 0.20 M CTAB was placed in a water bath (27 °C) and stirred at 1000 rpm. The seed particles were formed by the rapid addition of 0.60 mL of ice-cold aqueous 0.010 M $NaBH_4$. The resulting seed solution was stirred for 2 min and allowed to age for an additional 10 min prior to use. The growth solution in water was made by mixing 25 μL of 0.040 M $AgNO_3$, 5.0 mL of 0.20 M CTAB, 20 μL of 0.50 M H_2SO_4, 5.0 mL of 1.00 mM $HAuCl_4$, and 70 μL of 0.079 M ascorbic acid (note: the ascorbic acid must be prepared fresh and was added to the mixture last). After the addition of ascorbic acid, the growth solution was gently mixed until the color changed from dark yellow to colorless. Next, to the growth solution was added a 12 μL aliquot of the seed solution. The solution was then gently mixed again and incubated at 27 °C. The final growth solution was aged for a minimum of 2 h, in which the color of the solution changed from clear to light peach.

Synthesis of 3 nm Glutathione-Stabilized Gold Nanoparticles. The synthesis of small glutathione-capped Au nanoparticles was achieved with a slight modification from the published method.[24] Briefly, nanoparticles were synthesized by adding the reducing agent ($NaBH_4$) to a gold precursor ($HAuCl_4$) in the presence of a ligand, glutathione. A 1 mmol (0.39 g) of $HAuCl_4$ was dissolved in a solution of 30 mL of methanol and 20 mL of water, which resulted in a bright yellow solution. A 1 mmol (0.31 g) of glutathione is added to the rapidly stirred gold salt solution. The solution turned light brown and slowly turned colorless within 40 min. A $NaBH_4$ solution, freshly made by dissolving 5 mmol (0.19 g) of $NaBH_4$ in 40 mL of water, was slowly added to the vigorously stirred precursor solution, which caused the solution to immediately turn dark brown due to the formation of gold nanoparticles. The solution was quickly transferred into a water bath that was kept at 50 °C and stirring was continued for 1 h. The resulting solution was evaporated to near dryness on a rotary evaporator. Excess methanol was added to precipitate particles and wash reaction byproducts and any remaining starting material. The resulting solution was dialyzed in nanopure water for 72 h.

Preparation of Gold Nanoparticle−Graphene Oxide Hybrids. Graphene oxide solution was made by dispersing graphene oxide flakes in nanopure water. Graphene oxide flakes were not readily soluble in water, hence the mixture was sonicated for 30 min until the graphene oxide formed a homogeneous dispersion. The concentration of graphene oxide was 1 mg/mL. The graphene oxide dispersion in water exhibits long-term stability. Gold nanorods/nanoparticles were dissolved in water (∼1 mg/mL) forming homogeneous solutions. Graphene oxide and gold nanorods/nanoparticles were mixed at a 1:1 ratio (1 mL graphene oxide to 1 mL gold nanorod/nanoparticle solution) for 24 h. To maintain the amount of CTAB same for gold nanorods on graphene oxide, no purification step, besides the evaporation of solvent, was employed.

Heat Treatment of Gold Nanoparticle−Graphene Oxide Hybrids. The gold nanorods− and nanoparticle−graphene oxide hybrids were heated from 50 to 300 °C, at 50 °C increments using a Barnstead Thermolyne 1300 Furnace. Each sample was heated for 1 h in a glass vial in air. Solvents were removed to dryness before the particle samples were heated in powder form.

Characterization. UV−vis measurements of nanoparticle solutions were taken with a UV-2450 Shimadzu UV−vis spectrophotometer using quartz cells. Spectra were recorded from 800 to 200 nm (900 to 200 nm for gold nanorod solutions). Infrared spectra were taken with a PerkinElmer Spectrum 100 FT-IR spectrometer. Spectra were recorded from 4500 to 450 cm^{-1}. Transmission electron microscopy (TEM) images were taken with a JEOL 1200 EX II electron microscope operating at 90 keV. Samples dissolved in nanopure water were cast onto carbon-coated copper mesh grids and let dry for at least 30 min before analysis. Gold nanoparticle core sizes were analyzed with Scion Image Beta Release 2.0. Thermogravimetric analysis (TGA) measurements were performed on a SDT Q600 instrument using an ultrapurity nitrogen atmosphere (flow rate of 100 mL/min). Heating of the samples began at room temperature to 900 °C, with a heat rate of 20 °C/min.

DOI: 10.1021/am508801e
ACS Appl. Mater. Interfaces 2015, 7, 3406−3413

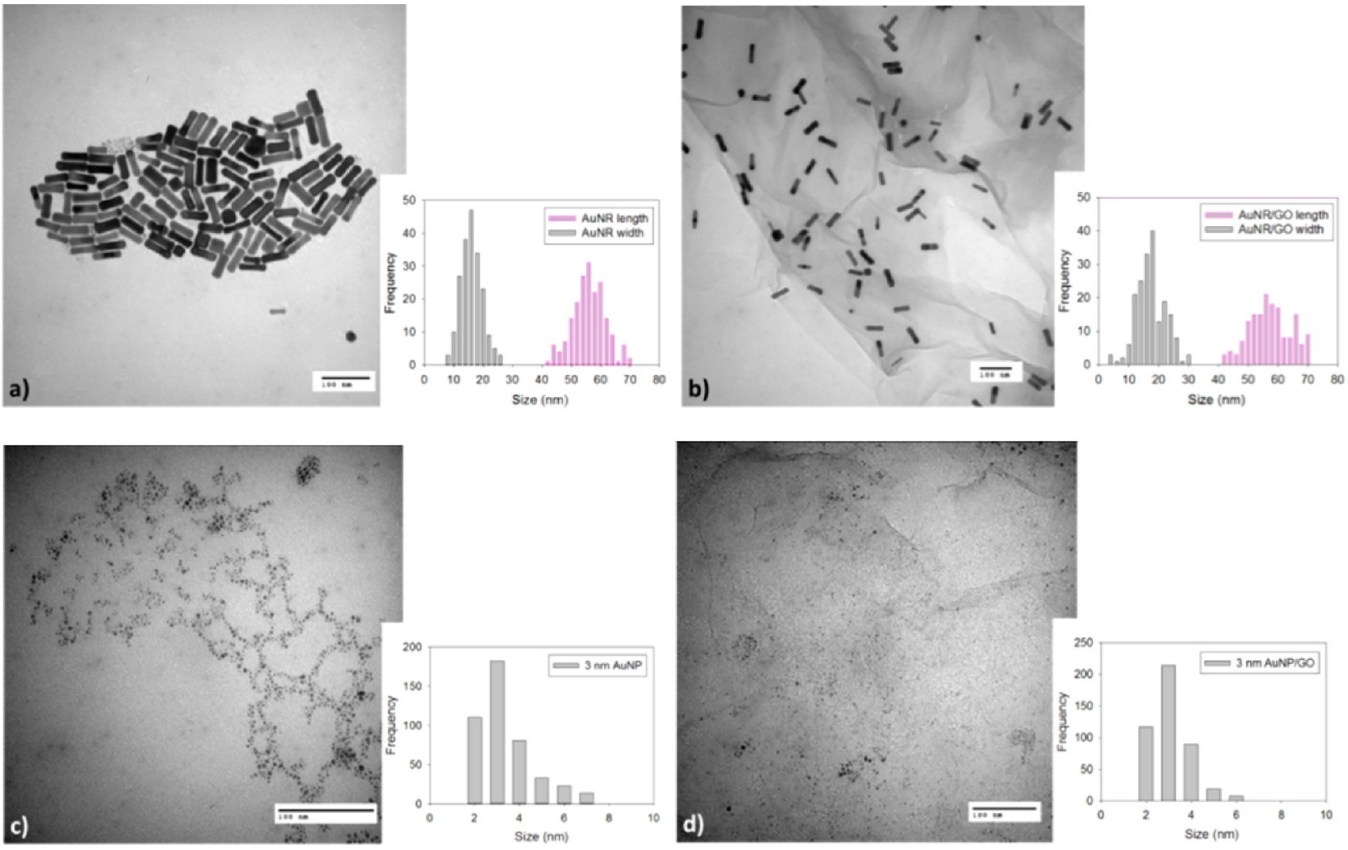

Figure 2. TEM images (size bars: 100 nm) and histograms of gold nanorods (a) before and (b) after the adsorption and 3 nm gold nanoparticles (c) before and (d) after the adsorption onto the surface of graphene oxide.

Table 1. Evolution of Average Core Sizes of Gold Nanorods and Nanoparticles Based on TEM Histogram Analyses

materials	gold nanorods (length/width or diameter)		gold nanoparticles (diameter)	
condition	free standing	assembled on graphene oxide	free standing	assembled on graphene oxide
room temp.	53.6 ± 8.2 nm 15.1 ± 3.6 nm (3.5)[a]	53.8 ± 13.2 nm 17.3 ± 6.3 nm (3.1)[a]	3.0 ± 1.4 nm	3.0 ± 1.0 nm
50 °C	58.2 ± 7.7 nm 23.4 ± 3.9 nm (2.5)[a]	89.4 ± 52.3 nm (1.0)[a]	3.2 ± 2.4 nm	3.1 ± 1.8 nm
100 °C	59.5 ± 9.1 nm 29.5 ± 3.9 nm (2.1)[a]	(1.0)[a]	3.5 ± 2.2 nm	3.3 ± 1.6 nm
150 °C	58.8 ± 8.5 nm 25.7 ± 5.1 nm (2.0)[a]	125.4 ± 52.0 nm (1.0)[a]	4.1 ± 2.3 nm	7.0 ± 3.6 nm
200 °C	(1.0)[a]	(1.0)[a]	8.0 ± 3.0 nm	10.1 ± 5.4 nm
250 °C			≥11.5 ± 5.3 nm[b]	≥11.0 ± 4.8 nm[b]
300 °C			≥12.2 ± 7.3 nm[b]	≥12.2 ± 4.7 nm[b]

[a]An aspect ratio (length/width) of gold nanorods. [b]For the histogram analysis of TEM images of gold nanoparticles heat-treated at 250 and 300 °C, the large irregularly shaped coalesced film-like structures were excluded from the analysis. Therefore, the actual average core size of produced metallic structures should be larger than the reported values in the table.

RESULTS AND DISCUSSION

Preparation of Gold Nanoparticle–Graphene Oxide Hybrids. The successful synthesis of the monodispersed gold nanorods dissolved in nanopure water was confirmed by UV–vis spectroscopy, which revealed the characteristic plasmon bands at 520 nm for the transverse electronic oscillation and at 780 nm for the longitudinal electronic oscillation (Figure 1a).[23] The result was in good agreement with the TEM image and histogram data showing that their length and width distributions of the majority of nanorods are ~54 nm in length and ~15 nm in width (Figure 2a), leading to an aspect ratio of ~3.5 to 1. The UV–vis spectra of Au nanoparticles exhibited a surface plasmon band of gold at 520 nm, which is particular to Au nanoparticles with similar core sizes (Figure 1b).[25] Figure 2c displays a TEM image of these gold nanoparticles along with histogram data, which revealed an average core size of 3.0 ± 1.4 nm.

Gold nanorods were self-assembled onto the surface of graphene oxide via electrostatic interactions between COOH/COO^- groups of graphene oxide and $(CH_3)_3N^+$ groups of bilayer CTAB-stabilized gold nanorods.[26−28] For gold nanoparticles, the noncovalent interactions (i.e., hydrogen bonding

DOI: 10.1021/am508801e
ACS Appl. Mater. Interfaces 2015, 7, 3406−3413

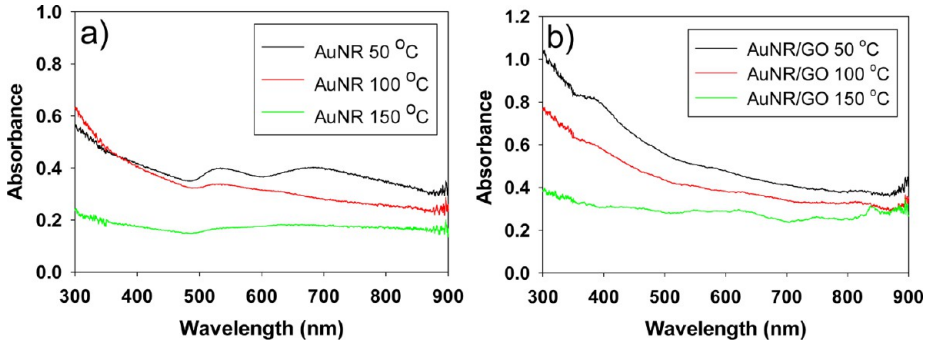

Figure 3. UV−vis spectra of (a) gold nanorods and (b) gold nanorod−graphene oxide hybrids heated at 50, 100, and 150 °C for 1 h.

and electrostatic interactions) between COOH or OH groups of graphene oxide and COO^- or NH_2 groups of glutathione ligands was the driving force for nanoparticle attachments to graphene oxide.[18,27−29]

After nanorods were adsorbed onto the surface of graphene oxide, the UV−vis spectra showed that the intensity of longitudinal plasmon band at 780 nm dramatically decreases, while the transverse plasmon band at 520 nm almost disappears (Figure 1a). The similar changes in the plasmon bands of gold nanorods, which are caused by the plasmon coupling between AuNRs adsorbed on the graphene oxide surface, have been previously observed by Liu et al.[26] When the 3 nm gold nanoparticles were adsorbed onto the graphene oxide surface, the plasmon band of gold at 520 nm also underwent an extensive broadening with a slight red shift as a result of the plasmon coupling between surface-assembled gold nanoparticles (Figure 1b).[29]

Table 1 summarizes the average core sizes and their respective standard deviations of the gold nanorods and nanoparticles before and after the adsorption onto the surface of graphene oxide. The results clearly demonstrated that the use of preformed nanoparticles afforded the retention of core size and dispersity of assembled nanoparticles without any significant change in their values. This confirms that graphene oxide does not change the size (or the shape) of gold nanorods and 3 nm gold nanoparticles or selectively deposit nanorods or nanoparticles with specific sizes or shape during the assembly processes. Therefore, this strategy of assembling preformed nanorods and nanoparticles directly onto the surface of graphene oxide would be an ideal method in controlling the size and morphology of the nanoparticles deposited on graphene oxide.

Heat Treatments of Gold Nanorods, Nanoparticles, and Graphene Oxide Hybrids. The heat-induced reshaping of gold nanorods or coarsening of gold nanoparticles, both free-standing and surface assembled, were monitored after the heat treatments of these materials at various temperatures. Figure 3 shows the UV−vis spectra of isolated free-standing gold nanorods heated at the temperatures ranging from 50 to 150 °C at 50 °C increments for 1 h. After heat treatment at 50 °C, the UV−vis spectra of gold nanorods (Figure 3a) showed that the surface plasmon bands at 520 and 780 nm have undergone dramatic changes from their original surface plasmon bands shown in Figure 1a (black). Especially, the plasmon band at 780 nm has significantly decreased in intensity and blue-shifted to lower wavelength (~680 nm). This shift indicated that the reshaping of gold nanorods has started to take place at this temperature. After heating at 100 °C, the plasmon bands at higher wavelength have almost disappeared in the UV−vis spectra. The complete disappearance of the surface plasmon bands at higher wavelength and the presence of visible plasmon band at ~520 nm suggested that the nanorods are continuously morphing into spherical particles, as the higher wavelength plasmon band is indicative of the longitudinal electronic oscillations. After the heat treatment at 200 °C, the gold nanorods became mostly insoluble in aqueous solvent and the UV−vis spectra of these particles no longer showed any significant absorption band.

For gold nanorods on graphene oxide, the UV−vis spectra of heated samples at 50 °C showed that the plasmon band at 780 nm observed for nonheated gold nanorod/graphene oxide hybrids (Figure 1a (red)) completely disappeared (Figure 3b). This indicated the gold nanorods on graphene oxide have undergone a rapid reshaping during heat treatments at even 50 °C. Heat treatments at higher temperature made the materials to lose their solubility in water, causing the absorbance of UV−vis spectra to decrease more with increased heating temperature.

TEM images of heated free-standing gold nanorods (Figure 4a−d) showed that the rods began to have a clear shape change after heating at 100 °C, transforming into rods with round edges. However, a careful histogram analysis of TEM images indicated that the gold nanorods have already begun to undergo some shape changes even after heating at 50 °C. Table 1 provides an average size and aspect ratio analysis of heated gold nanorods. Both average length and width of gold nanorods were increased after heat treatments at 50 °C, suggesting that the reshaping process also involved some coarsening of nearby nanorods. The decrease in aspect ratio from 3.5 to 2.5 clearly indicated the shape change of nanorods to spherical particles has started to take place at this temperature. The smaller aspect ratio of nanorods corresponded very well with the UV−vis spectra, which show the blue shifts (from 780 to 680 nm) of surface plasmon bands of gold nanorods (Figure 3a).[30−33] The aspect ratio of gold nanorods further decreased to 2.1 after heat treatments at 100 °C, indicating additional reshaping of nanorods. This change was due mostly to the further increase in the width of nanorods, becoming particles with more round-shaped edges. After heat treatment at 150 °C, spherical particles began to appear, as seen in the TEM image shown in Figure 4c. Heat treatments at 200 °C transformed all nanorods into spherical particles (Figure 4d). It has been shown that aqueous gold nanorods would undergo reshaping into large spherical particles after heating, because a sphere is the most thermodynamically favored particle shape with the lowest surface energy.[30] Any other shaped particles such as bent and twisted nanorods and φ-shaped particles (nanorods with a

DOI: 10.1021/am508801e
ACS Appl. Mater. Interfaces 2015, 7, 3406−3413

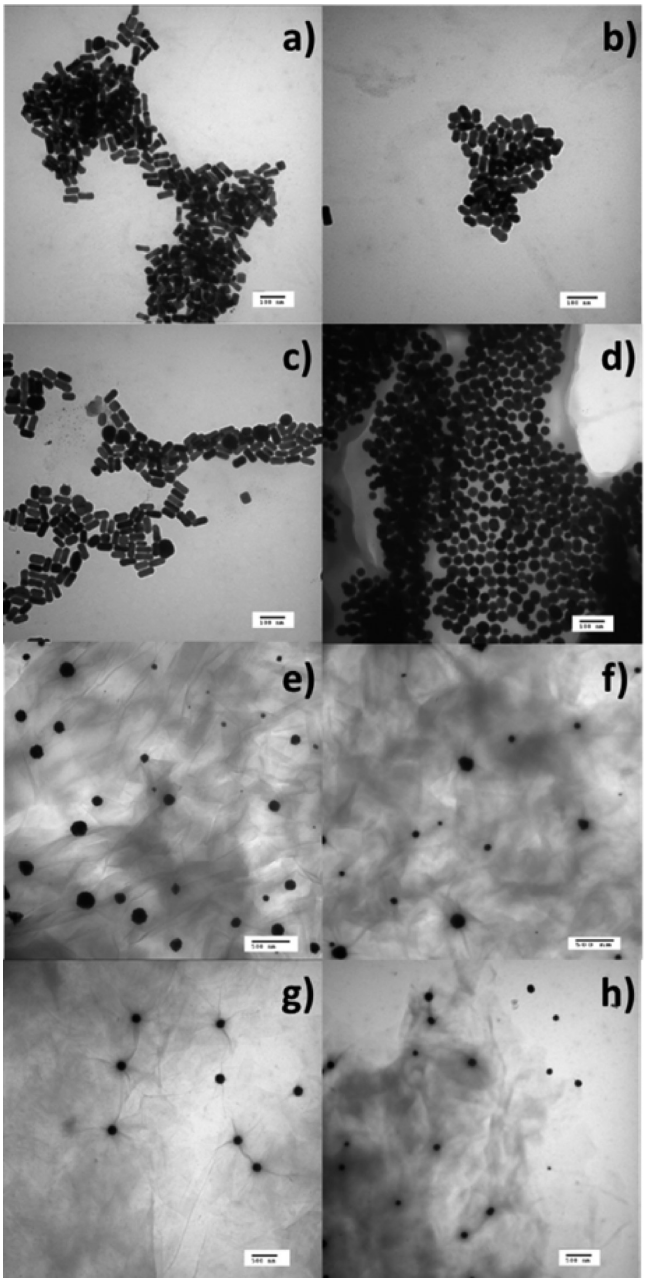

Figure 4. TEM images of free-standing gold nanorods (scale bar = 100 nm) heated at (a) 50 °C, (b) 100 °C, (c) 150 °C, and (d) 200 °C for 1 h and gold nanorods on graphene oxide (scale bar = 500 nm) heated at (e) 50 °C, (f) 100 °C, (g) 150 °C, and (h) 200 °C for 1 h. Note the size bars of images g/h and e/f are not in the same lengths.

convex deformation in the middle) were not produced as the intermediates during the reshaping process.[33,34]

For gold nanorods assembled on graphene oxide, TEM results showed that nanorods underwent a complete shape change to spherical nanoparticles after the heat treatments at only 50 °C (Figure 4e). No other shape change was observed from the nanorod−graphene oxide hybrids heated at the higher temperature (Figure 4f−h). Table 1 shows the average sizes and aspect ratios of heated gold nanorods on graphene oxide at different temperatures. The histogram analysis confirms that the dramatic changes in the aspect ratio took place after heating the gold nanorods−graphene oxide hybrids at 50 °C. Compared to the reshaping process of free-standing gold nanorods, which required the temperature of 200 °C for the complete reshaping to spherical nanoparticles, the reshaping of surface assembled gold nanorods was clearly promoted by the presence of graphene oxide.

It has been known that the reshaping of nanorods largely depends on the surface condition of the nanorods. When the CTAB-stabilized nanorods dissolved in aqueous solvents are heated, CTAB acts as a protective layer for heat diffusion at the lower temperature.[35] However, at the higher temperature, the encapsulation of thermal energy in the CTAB layers causes the disruption of stabilizing ligands and the subsequent reshaping of nanorods in aqueous environment. The direct comparison of the heat treatments of the free-standing gold nanorods and the gold nanorod-graphene oxide hybrids suggested that the disruption of CTAB layers would be facilitated with the presence of graphene oxide. Graphene oxide interacts strongly with the CTAB ligands of the gold nanorods,[26] which is evidenced by the facile self-assembly of nanorods onto the surface of graphene oxide. With its well-known flexibility,[36] graphene oxide should be able to partially bend around gold nanorods during the heat treatments to maximize chemical interactions with the CTAB ligands on nanorod surfaces. The CTAB ligands are then pulled away from the surface of nanorods and placed under the equilibrium, traveling between nanorods and graphene oxide. Some CTAB ligands would undergo spillover on graphene oxide and may become permanently desorbed from the surface of gold nanorods, making gold nanorods more venerable for the reshaping. Scheme 1 shows the proposed nanorod reshaping mechanism facilitated by the presence of graphene oxide.

In addition to the comparison of the free-standing gold nanorods with the graphene oxide surface-immobilized gold nanorods, which showed the significant influence of graphene oxide on the nanorod reshaping mechanism, the coarsening behaviors of both the free-standing and the surface-assembled small gold nanoparticles were investigated. Figure 5a shows the UV−vis spectra of free-standing 3 nm gold nanoparticles after heat treatments at the temperature ranging from 50 to 300 °C. The results suggested that the surface plasmon bands of gold nanoparticles started to red-shift at the heating temperature between 150 and 200 °C. The decrease in the intensity of surface plasmon bands was only observed after heat treatments at 150 °C and was continued until the heating temperature was at 200 °C. This result indicated that the free-standing gold nanoparticles were mostly stable and were without significant property changes until the particles were heated at 150 °C, at which the particles started to aggregate and become partially insoluble. For the nanoparticles heated at higher temperatures (200, 250, and 300 °C), completely different spectral features were observed from UV−vis spectra, which resemble the characteristic of localized metallic film-like structures.[37,38] Further investigation with heat treatments at the temperature increments of 10 °C in the range between 160 and 190 °C indicated the transition between particle-like optical responses to film-like ones took place at the heating temperature of 170 °C (Figure S1, Supporting Information).

TEM images of the free-standing gold nanoparticles and surface-immobilized gold nanoparticles on graphene oxide after the heat treatments at 100, 200, and 300 °C are shown in Figure 6. The changes in the average core size of gold nanoparticles along with standard deviation for samples heated at temperatures between 50 and 200 °C are also summarized in Figure 7. The core size and the distribution of samples heated

DOI: 10.1021/am508801e
ACS Appl. Mater. Interfaces 2015, 7, 3406−3413

Scheme 1. Proposed Gold Nanorod Reshaping Mechanism for Nanorod−Graphene Oxide Hybrids

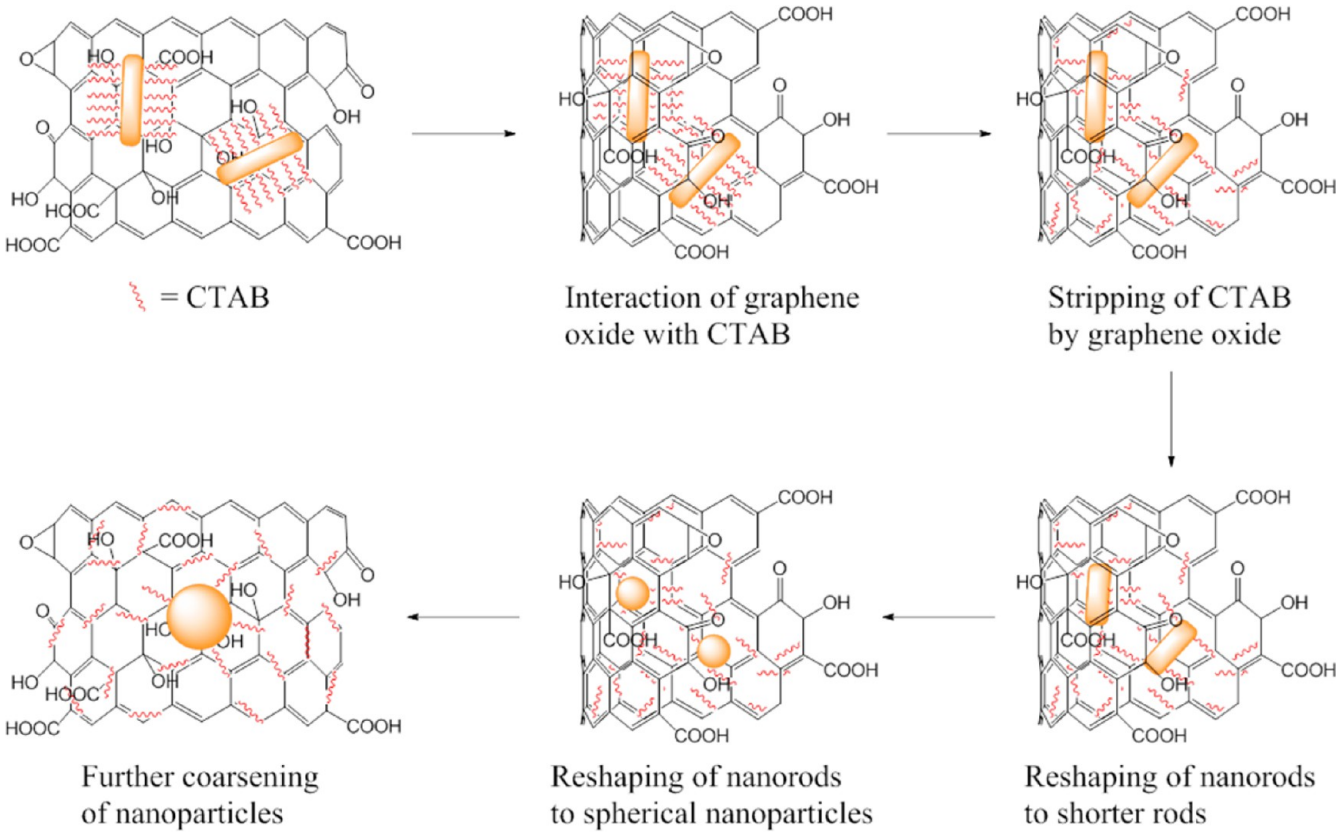

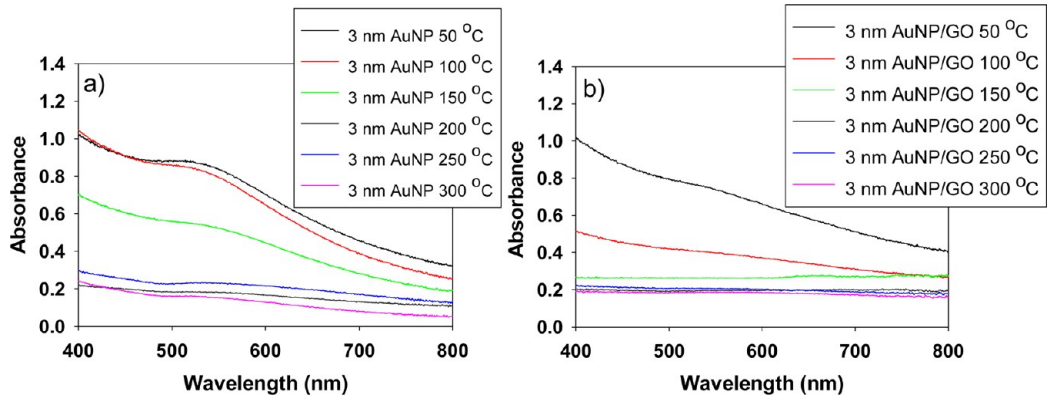

Figure 5. UV−vis spectra of heated (a) 3 nm gold nanoparticles and (b) gold nanoparticles on graphene oxide at 50−300 °C.

at 250 and 300 °C were not included in this figure, because the exclusion of the large irregularly shaped coalesced film-like structures from the TEM analysis caused the actual sizes to be undervalued and inaccurate.

Table 1 also summarizes the evolutions in the average core sizes of free-standing gold nanoparticles and gold nanoparticle−graphene oxide hybrids after heat treatments at various temperatures. The most significant increases in the average core size of the free-standing gold nanoparticles occurs after the heat treatments at the temperature between 150 and 200 °C, from 4.2 ± 2.3 to 8.0 ± 3.0 nm. In comparison, the dramatic increases in average core sizes for surface-immobilized gold nanoparticles on graphene oxide took place after the heat treatments at the temperature between 100 to 150 °C, from 3.3 ± 1.6 to 7.0 ± 3.6 nm. This trend identified from the heat treatments of spherical gold nanoparticles also suggested the influence of graphene oxide during the coarsening of small 3 nm gold nanoparticles. The gold nanoparticles on graphene oxide samples underwent a much faster coarsening and a greater core size transition at the lower temperature, suggesting the presence of the interaction of glutathione ligands on gold nanoparticles with the oxygenated surface of graphene oxide. This strong interaction with graphene oxide caused the subsequent disruption and desorption of surrounding glutathione ligands from the gold nanoparticle surfaces and facilitated the aggregation and coarsening of gold nanoparticles at the lower temperature.

CONCLUSION

For both gold nanorods and nanoparticles, the shape and/or core size evolutions of gold nanorods and nanoparticles were greatly affected by the presence of graphene oxide supports.

DOI: 10.1021/am508801e
ACS Appl. Mater. Interfaces 2015, 7, 3406−3413

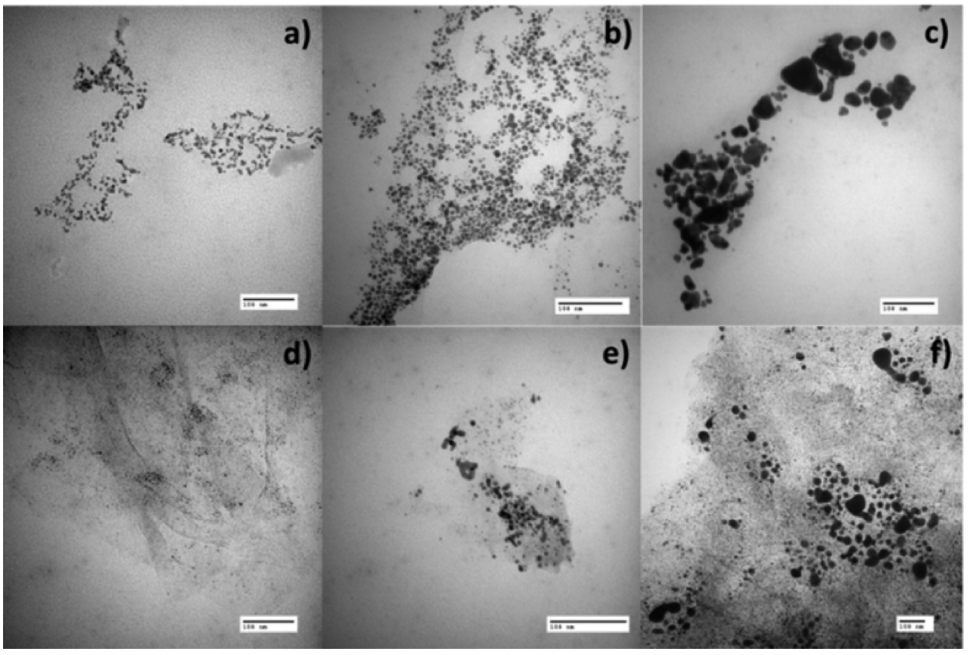

Figure 6. TEM images (size bars = 100 nm) of heated 3 nm gold nanoparticles at (a) 100 °C, (b) 200 °C, and (c) 300 °C and gold nanoparticles on graphene oxide at (d) 100 °C, (e) 200 °C, and (f) 300 °C.

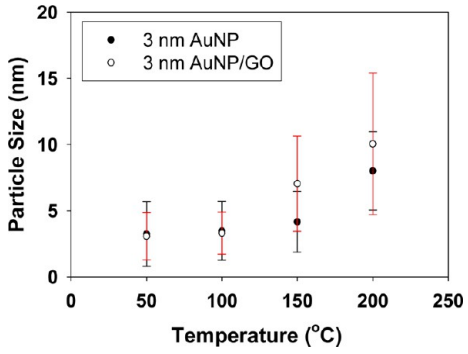

Figure 7. Evolution of average core size and distribution of heated gold nanoparticles and nanoparticles on graphene oxide. Black error bars correspond to 3 nm gold nanoparticles and red error bars correspond to 3 nm gold nanoparticles on graphene oxide.

Despite being known as an excellent template for the postassembly and growing of nanoparticles, our results demonstrated that graphene oxide would lower the stability of assembled metallic nanostructures by disrupting and stripping the protecting organic ligands from the surface of nanomaterials such as gold nanorods and nanoparticles especially during the heat treatments. This is against the typical prediction on the stability of the assembled metal nanostructures when they are deposited on solid supports. Such a facile thermally induced transformation of nanomaterial-graphene oxide hybrids indicates that their technological applications including catalysis and electronic/optical devices would require the development of new strategies for enhancing their overall stability.

■ ASSOCIATED CONTENT

Ⓢ Supporting Information

UV−vis spectra of gold nanoparticles heated from 160 to 190 °C (Figure S1), additional TEM images (Figure S2), and other supporting characterization data including FT-IR (Figure S3) and TGA (Figure S4). This material is available free of charge via the Internet at http://pubs.acs.org.

■ AUTHOR INFORMATION

Corresponding Author

*Y.-S. Shon. E-mail: ys.shon@csulb.edu.

Author Contributions

The paper was written through contributions of all authors. All authors have given approval to the final version of the paper.

Funding

This research was funded by grants from the National Institute of Health and CSULB.

Notes

The authors declare no competing financial interest.

■ ACKNOWLEDGMENTS

The authors thank Tom Douglas for the help with TEM analysis and the National Institute of General Medical Science (#SC3GM089562) for financial support.

■ REFERENCES

(1) Yin, P. T.; Kim, T.-H.; Choi, J.-W.; Lee, K.-B. Prospects for Graphene-Nanoparticle-based Hybrid Sensors. *Phys. Chem. Chem. Phys.* **2013**, *15*, 12785−12799.

(2) Sun, S.; Wu, P. Easy Fabrication of Macroporous Gold Films Using Graphene Sheets as a Template. *ACS Appl. Mater. Interfaces* **2013**, *5*, 3481−3486.

(3) Ismaili, H.; Geng, D.; Sun, A. X.; Kantzas, T. T.; Workentin, M. S. Light-Activated Covalent Formation of Gold Nanoparticle-Graphene and Gold Nanoparticle-Glass Composites. *Langmuir* **2011**, *27*, 13261−13268.

(4) Tan, C.; Huang, X.; Zhang, H. Synthesis and Applications of Graphene-based Nobel Metal Nanostructures. *Mater. Today* **2013**, *16*, 29−36.

(5) Hong, W.; Bai, H.; Xu, Y.; Yao, Z.; Gu, Z.; Shi, G. Preparation of Gold Nanoparticle/Graphene Composites with Controlled Weight Contents and Their Application in Biosensors. *J. Phys. Chem. C* **2010**, *114*, 1822−1826.

DOI: 10.1021/am508801e
ACS Appl. Mater. Interfaces 2015, 7, 3406−3413

(6) Pyun, J. Graphene Oxide as Catalyst: Application of Carbon Materials beyond Nanotechnology. *Angew. Chem., Int. Ed.* **2011**, *50*, 46−48.
(7) Dhakshinamoorthy, A.; Alvaro, M.; Concepción, P.; Fornés, V.; Garcia, H. Graphene Oxide as an Acid Catalyst for the Room Temperature Ring Opening of Epoxides. *Chem. Commun.* **2012**, *48*, 5443−5445.
(8) Gao, Y.; Ma, D.; Wang, C.; Guan, J.; Bao, X. Reduced Graphene Oxide as a Catalyst for Hydrogenation of Nitrobenzene at Room Temperature. *Chem. Commun.* **2011**, *47*, 2432−2434.
(9) Varela-Rizo, H.; Martin-Gullön, I.; Terrones, M. Hybrid Films with Graphene Could Now Replace Indium Tin Oxide. *ACS Nano* **2012**, *6*, 4565−4572.
(10) Hrbek, J.; Hoffmann, F. M.; Park, J. B.; Liu, P.; Stacchiola, D.; Hoo, Y. S.; Ma, S.; Nambu, A.; Rodriguez, J. A.; White, M. G. Adsorbate-Driven Morphological Changes of a Gold Surface at Low Temperature. *J. Am. Chem. Soc.* **2008**, *130*, 17272−17273.
(11) Sugden, M. W.; Richardson, T. H.; Leggett, G. Sub-10 Ω Resistance Gold Films Prepared by Removal of Ligands from Thiol-Stabilized 6 nm Gold Nanoparticles. *Langmuir* **2010**, *26*, 4331−4338.
(12) Risse, T.; Shaikhutdinov, S.; Nilius, N.; Sterrer, M.; Freund, H.-J. Gold Supported on Thin Oxide Films: From Single Atoms to Nanoparticles. *Acc. Chem. Res.* **2008**, *41*, 949−956.
(13) Bauer, M.; Schoch, R.; Shao, L.; Zhang, B.; Knop-Gericke, A.; Willinger, M.; Schlögl, R.; Teschner, D. Structure-Activity Studies on Highly Active Palladium Hydrogenation Catalysts by X-ray Absorption Spectroscopy. *J. Phys. Chem. C* **2012**, *116*, 22375−22385.
(14) Huang, H.; Wang, X. Recent Progress on Carbon-based Support Materials for Electrocatalysts of Direct Methanol Fuel Cells. *J. Mater. Chem. A* **2014**, *2*, 6266−6291.
(15) Karousis, N.; Tsotsou, G.-E.; Evangelista, F.; Rudolf, P.; Ragoussis, N.; Tagmatarchis, N. Carbon Nanotubes Decorated with Palladium Nanoparticles: Synthesis, Characterization, and Catalytic Activity. *J. Phys. Chem. C* **2008**, *112*, 13463−13469.
(16) Gopiraman, M.; Babu, S. G.; Khatri, Z.; Kai, W.; Kim, Y. A.; Endo, M.; Karvembu, R.; Kim, I. S. Dry Synthesis of Easily Tunable Nano Ruthenium Supported on Graphene: Novel Nanocatalysts for Aerial Oxidation of Alcohols and Transfer Hydrogenation of Ketones. *J. Phys. Chem. C* **2013**, *117*, 23582−23596.
(17) Cano, M.; Benito, A. M.; Urriolabeitia, E. P.; Arenal, R.; Maser, W. K. Reduced Graphene Oxide: Firm Support for Catalytically Active Palladium Nanoparticles and Game Changer in Selective Hydrogenation Reactions. *Nanoscale* **2013**, *5*, 10189−10193.
(18) Bae, H. S.; Seo, E.; Jang, S.; Park, K. H.; Kim, B.-S. Hybrid Gold Nanoparticle-Reduced Graphene Oxide Nanosheets as Active Catalysts for Highly Efficient Reduction of Nitroarenes. *J. Mater. Chem.* **2011**, *21*, 15431−15436.
(19) Salam, N.; Sinha, A.; Roy, A. S.; Mondal, P.; Jana, N. R.; Islam, S. M. Synthesis of Silver-Graphene Nanocomposite and Its Catalytic Application for the One-Pot Three-Component Coupling Reaction and One-Pot Synthesis of 1,4-Disubstituted 1,2,3-Triazoles in Water. *RSC Adv.* **2014**, *4*, 10001−10012.
(20) Dash, P.; Bond, T.; Fowler, C.; Hou, W.; Coombs, N.; Scott, R. W. J. Rational Design of Supported PdAu Nanoparticle Catalysts from Structured Nanoparticle Precursors. *J. Phys. Chem. C* **2009**, *113*, 12719−12730.
(21) Adijanto, L.; Sampath, A.; Yu, A. S.; Cargnello, M.; Fornasiero, P.; Gorte, R. J.; Vohs, J. M. Synthesis and Stability of Pd@CeO_2 Core-Shell Catalyst in Solid Oxide Fuel Cells Anodes. *ACS Catal.* **2013**, *3*, 1801−1809.
(22) Du, M.; Sun, D.; Yang, H.; Huang, J.; Jing, X.; Odoom-Wubah, T.; Wang, H.; Jia, L.; Li, Q. Influence of Au Particle Size on Au/TiO_2 Catalysts for CO Oxidation. *J. Phys. Chem. C* **2014**, *118*, 19150−19157.
(23) Castellana, E. T.; Gamez, R. C.; Russell, D. H. Label-Free Biosensing with Lipid-Functionalized Gold Nanorods. *J. Am. Chem. Soc.* **2011**, *133*, 4182−4185.
(24) Stamplecoskie, K. G.; Chen, Y.-S.; Kamat, P. V. Excited-State Behavior of Luminescent Glutathione-Protected Gold Clusters. *J. Phys. Chem. C* **2014**, *118*, 1370−1376.
(25) Cheng, P. P. H. C.; Silvester, D.; Wang, G.; Kalyuzhny, G.; Douglas, A.; Murray, R. W. Dynamic and Static Quenching of Fluorescence by 1−4 nm Diameter Gold Monolayer-Protected Clusters. *J. Phys. Chem. B* **2006**, *110*, 4637−4644.
(26) Hu, C.; Rong, J.; Cui, J.; Yang, Y.; Yang, L.; Wang, Y.; Liu, Y. Fabrication of a Graphene Oxide-Gold Nanorod Hybrid Material by Electrostatic Self-Assembly for Surface-Enhanced Raman Scattering. *Carbon* **2013**, *51*, 255−264.
(27) Zedan, A. F.; Moussa, S.; Terner, J.; Atkinson, G.; El-Shall, M. S. Ultrasmall Gold Nanoparticles Anchored to Graphene and Enhanced Photothermal Effects by Laser Irradiation of Gold Nanostructures in Graphene Oxide Solutions. *ACS Nano* **2013**, *7*, 627−636.
(28) Xu, C.; Yang, D.; Mei, L.; Lu, B.; Chen, L.; Li, Q.; Zhu, H.; Wang, T. Encapsulating Gold Nanoparticles or Nanorods in Graphene Oxide Shells as a Novel Gene Vector. *ACS Appl. Mater. Interfaces* **2013**, *5*, 2715−2724.
(29) Dervishi, E.; Bourdo, S.; Driver, J. A.; Watanabe, F.; Biris, A. R.; Ghosh, A.; Berry, B.; Saini, V.; Biris, A. S. Catalytic Conversion of Graphene into Carbon Nanotubes vis Gold Nanoclusters at Low Temperatures. *ACS Nano* **2012**, *6*, 501−511.
(30) Mohamed, M. B.; Ismail, K. Z.; Link, S.; El-Sayed, M. A. Thermal Reshaping of Gold Nanorods in Micelles. *J. Phys. Chem. B* **1998**, *102*, 9370−9374.
(31) Link, S.; Burda, C.; Nikoobakht, B.; El-Sayed, M. A. Laser-Induced Shape Changes of Colloidal Gold Nanorods Using Femtosecond and Nanosecond Laser Pulses. *J. Phys. Chem. B* **2000**, *104*, 6152−6163.
(32) Al-Sherbini, E.-S. A. M. UV-visible Light Reshaping of Gold Nanorods. *Mater. Chem. Phys.* **2010**, *121*, 349−353.
(33) Gordel, M.; Olesiak-Banska, J.; Matczyszyn, K.; Nogues, C.; Buckle, M.; Samoc, M. Post-Synthesis Reshaping of Gold Nanorods Using a Femtosecond Laser. *Phys. Chem. Chem. Phys.* **2014**, *16*, 71−78.
(34) Nikoobakht, B.; El-Sayed, M. A. Preparation and Growth mechanism of Gold Nanorods (NRs) Using Seed-Mediated Growth Method. *Chem. Mater.* **2003**, *15*, 1957−1962.
(35) Horiguchi, Y.; Honda, K.; Kato, Y.; Nakashima, N.; Niidome, Y. Photothermal Reshaping of Gold Nanorods Depends on the Passivating Layers of the Nanorod Surfaces. *Langmuir* **2008**, *24*, 12026−12031.
(36) Kim, M.; Lee, C.; Jang, J. Fabrication of Highly Flexible, Scalable, and High-Performance Supercapacitors Using Polyaniline/Reduced Graphene Oxide Film with Enhanced Electrical Conductivity and Crystallinity. *Adv. Funct. Mater.* **2014**, *24*, 2489−2499.
(37) Shon, Y.-S.; Aquino, M.; Pham, T. V.; Rave, D.; Ramirez, M.; Lin, K.; Vaccarello, P.; Lopez, G.; Gredig, T.; Kwon, C. Stability and Morphology of Gold Nanoisland Arrays Generated from Layer-by-Layer Assembled Nanoparticle Multilayer Films: Effects of Heating Temperature and Particle Size. *J. Phys. Chem. C* **2011**, *115*, 10597−10605.
(38) Vaccarello, P.; Tran, L.; Meinen, J.; Kwon, C.; Abate, Y.; Shon, Y.-S. Characterization of Localized Surface Plasmon Resonance Transducers Produced from Au_{25} Nanoparticle Multilayers. *Colloids Surf., A* **2012**, *402*, 146−151.

DOI: 10.1021/am508801e
ACS Appl. Mater. Interfaces 2015, 7, 3406−3413